01 Jan 2023

Challenges and Prospects of Vehicle OTA Spherical Near-Field Measurement Probes

Dao Lin

Zhanghua Cai

Lidong Chi

Fuhai Li

et. al. For a complete list of authors, see https://scholarsmine.mst.edu/ele_comeng_facwork/5166

Recommended Citation

D. Lin et al., "Challenges and Prospects of Vehicle OTA Spherical Near-Field Measurement Probes," *2023 IEEE Symposium on Electromagnetic Compatibility and Signal/Power Integrity, EMC+SIPI 2023*, pp. 100 - 104, Institute of Electrical and Electronics Engineers, Jan 2023.
The definitive version is available at https://doi.org/10.1109/EMCSIPI50001.2023.10241662

2023 IEEE Symposium on Electromagnetic Compatibility & Signal/Power Integrity (EMC+SIPI) | 979-8-3503-0976-8/23/$31.00 ©2023 IEEE | DOI: 10.1109/EMCSIPI50001.2023.10241662

Challenges and Prospects of Vehicle OTA Spherical Near-Field Measurement Probes

Dao Lin
Electrical and Information Engineering
Hunan University
Chang sha, China,
983888755@hnu.edu.cn

Zhanghua Cai, Student Member, IEEE
LinkE Technologies Co., Ltd.
Zhuhai, China,
Zhanghua.cai@generaltest.com

Lidong Chi, Student Member, IEEE
LinkE Technologies Co., Ltd.
Zhuhai, China,
565548254@qq.com

Fuhai Li, Senior Member, IEEE
Electrical and Information Engineering Department
Hunan University
Chang sha, China,
lifuhai@hnu.edu.cn

James L. Drewniak, Fellow, IEEE
Missouri University of Science and Technology
Rolla, MO, USA
drewniak@mst.edu

Gang Feng, Member, IEEE
Missouri University of Science and Technology
Rolla, MO, USA
gang.feng@linketech.cn

Yihong Qi, Fellow, IEEE
LinkE Technologies Co., Ltd.
Zhuhai, China
yihongqi@gmail.com

***Abstract*—This paper discusses the issue of measuring probe indicators for large-scale equipment, such as automobiles, under conditions of offset configuration. A simulation of spherical near-field measurement based on an offset configuration is presented in this paper. The measurement error is defined according to the reference data calculated by spherical wave expansion theory. Through comparative analysis of the simulation results, the main reason for the measurement error is the insufficient coverage of the probe's beamwidth. By adjusting the probe's radiation pattern using simulation software, an optimized probe that satisfies near-field measurement requirements under meter-level offset conditions is obtained. Finally, based on the simulation results, a set of recommended values for the main performance of the optimized probe is provided.**

Keywords—spherical near-field measurement, offset measurement, probe indexes

I. Introduction

With the rapid development of wireless communication technology, smart cars equipped with vehicle-to-everything (V2X) technology, and unmanned boats supporting 5G or even 6G communication systems, have emerged one after another. While providing great convenience for people's daily lives, their safety and reliability have also received increasing attention. Like other wireless communication devices, large products such as cars and boats need to undergo rigorous radiation performance measurements before they can be marketed. Designing and calculating the vehicle frame model with simulation software is complicated. Therefore, the most straightforward and efficient way to determine radiation performance is through near-field measurements [1]. To meet the functional requirements of intelligent automobiles, there has been a significant increase in the types and number of antennas installed on the automobile frame. Antennas are no longer limited to the car roof but can be distributed on both sides of the car body, the rear, and even along the edges of the windows. According to the definition of near-field measurement, to obtain accurate near-field sampling data, the entire Device Under Test (DUT) should be enclosed within a sampling sphere centered on itself with a minimum radius [2-3].

When conducting spherical near-field measurements on large objects such as cars, it is common for the Antenna Under Test (AUT) to be in an offset position relative to the measurement center. This is because of the DUT's large size and certain mechanical constraints of the measurement system, such as the limited mobility of the positioning devices and turntables in an anechoic chamber. Similarly, the measurement probe typically follows a fixed trajectory, and its orientation is also fixed, pointing only towards the measurement center of the system [2-5].

In this case, traditional near-field measurement probes may not guarantee the accuracy requirements for offset measurements. Fig. 1 illustrates one possible scenario of the offset configuration in automotive near-field measurements. The AUT is mounted at the rear of the car, while the car is placed in the center of the measurement system's turntable, with the measurement probe always pointing towards the center of the system. In this situation, the half-power beamwidth of the measurement probe is relatively poor, and the main lobe cannot cover the AUT. In the worst case, the null of the measurement probe's radiation pattern is aligned with the AUT, resulting in very low electromagnetic energy at the sampling point. As a result, the sampled data error is large, and even the sampled data is the system noise. The near-field data cannot be accurately sampled, and even post-processing of the data (such as probe compensation) yields little effect in diminishing measurement errors. This error is due to the limitation of the probe performance, which cannot sample outside the beamwidth range due to the offset configuration, rather than the positioning deviation of the probe. Moreover, if the symmetry of the measurement probe's beam is poor, there will be significant deviations in the sampling values at the same distance as the DUT rotates horizontally with the turntable. This deviation can cause significant problems in processing the sampled data. Additionally, the cross-polarization performance of the measurement antenna may also affect the accuracy of the near-field sampling data. If the polarization mismatch

phenomenon in the direction of the AUT is severe, it will cause significant interference to the sampling results. The aforementioned problems directly affect the accuracy of the sampling, and the resulting error is difficult to eliminate by algorithm.

The preceding analysis highlights the difference in performance requirements for probe antennas when conducting offset near-field measurements. In order to ensure the accuracy of the sampling data under the offset configuration, more stringent requirements should be put forward for the radiation performance of the probe antenna. However, currently, research on near-field measurement probes for large DUTs is limited. Especially for the offset configuration at the meter level, there are no clear reference standards for probe antenna performance.

The purpose of this paper is to investigate the performance requirements of measurement probes under the offset configuration. Section II provides a detailed introduction to the definition of near-field and far-field transformations and the theory of spherical wave expansion. Section III describes the experimental setup and process, including the discussion and analysis of the experimental results obtained from offset near-field measurement simulations. Section IV elucidates the bandwidth issue in high-frequency near-field measurement probe design, and the radiation pattern of the probe is adjusted using simulation software to ultimately obtain a set of recommended probe performance indicators

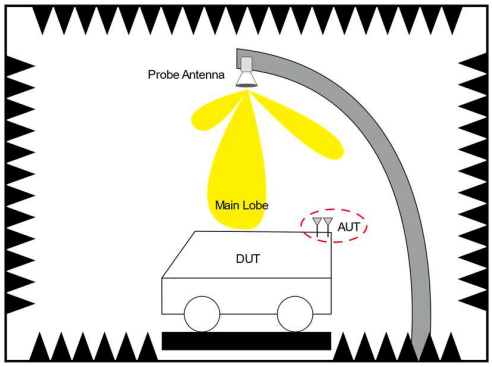

Fig. 1.Near-field measurement in an offset situation

that can meet the actual needs of the offset near-field measurement.

II. Near-Field-to-Far-Field Transformation and Spherical Wave Expansion Theory

The performance of an antenna is typically evaluated based on its electromagnetic radiation capability in the far-field (FF). However, the near-field (NF) also plays an important role in the process of electromagnetic wave propagation, as it refers to the region in close proximity to the radiation source $(R < 2D^2/\lambda)$. In contrast, the FF region is relatively far away from the radiation source $(R > 2D^2/\lambda)$[2-5]. The near-field-to-far-field (NF/FF) transformation is a mathematical vector transformation [1]. The complex NF and simple FF field vectors conversion can be realized through mathematical formula deduction. As a result, the NF and FF of electromagnetic field theory are connected. To obtain FF antenna characteristics from the NF radiation patterns sampled in such facilities, a NF/FF transformation is required [6-7].

This transformation involves the use of a spherical wave expansion (SWE) technique, which is a well-established method for performing NF/FF transformations in conventional spherical near-field sampling configurations [6]. In other words, it allows relatively easy-to-measure NF sampling data to be converted into directly usable FF data. The schematic diagram and actual image of a spherical NF measurement system are shown in Fig. 2 and Fig. 3, respectively.

Taking the Cartesian coordinate system as an example. If the probe antenna is located at a point $P(x_p, y_p, z_p)$ on the sphere, and the DUT is located at another point $M(x_m, y_m, z_m)$. According to the transmission equation of the spherical NF transform [6], the received signal strength w can be described by the following (1)-(4):

$$w(A,\chi,\theta,\phi) = \sum_{\substack{smn \\ \mu}} Q_{smn} \cdot e^{im\phi} d^n_{\mu m}(\theta) e^{im\chi} \cdot P_{s\mu n}(kA) \tag{1}$$

$$A = \sqrt{(x_p - x_m)^2 + (y_p - y_m)^2 + (z_p - z_m)^2} \tag{2}$$

$$Q_{smn} = v \cdot T_{smn} \tag{3}$$

$$P_{s\mu n}(kA) = \frac{1}{2} \sum_{\sigma v} C^{sn}_{\sigma\mu v}(kr)\, R_{\sigma\mu v} \tag{4}$$

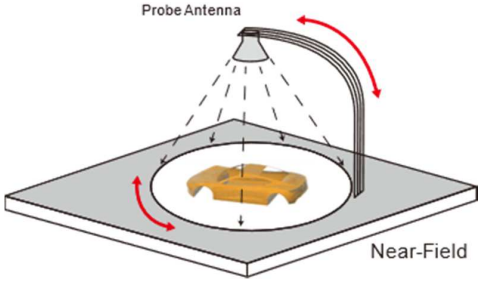

Fig. 2.Spherical near-field measurement schematic

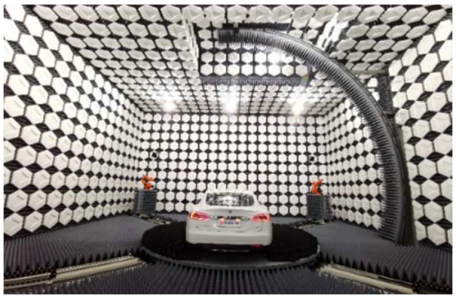

Fig. 3.Spherical near-field measurement actual image

A denotes the preset measurement distance, χ is the polarization rotation angle between the probe and the DUT, and (θ, ϕ) denotes the pitch and azimuth angles at the probe's location at point P. v is the strength of the transmitted signal. The complex amplitudes of the spherical mode coefficients

Q_{smn} have three indexes: degree n, order $m \leq n$, and $s \in \{1, 2\}$ [6]. The index s is connected to the components of the transverse electric and transverse magnetic waves [6]. The index m describes the azimuth variation of the field [6]. The degree n takes values satisfying $n \leq N, n \in Z$. The N inside is the maximal mode associated to the wavelength and the minimum spherical radius of the wrapped DUT. The second term $e^{im\phi} d^n_{\mu m}(\theta) e^{im\chi}$ is the rotation factor in the spherical wave extension. The last term $P_{s\mu n}(kA)$ is defined as the response constant of the probe, including the translation coefficient of the spherical wave and the probe reception coefficient. The only unknown variable in the equation is Q_{smn}, and once it is solved for, the coefficient Q_{smn} can be substituted into the spherical wave expansion. When the SWE is applied, the measured spherical NF is projected over a set of orthogonal spherical wave functions computing the spherical wave coefficients (SWC) [6]. The FF is then evaluated combining the SWC with the spherical wave functions computed at an infinite distance from the origin [6].

III. Vehicle OTA Measurement Antenna Simulation

The entire vehicle should be considered as a part of the test object because the common mode currents from the antenna flow through the vehicle, making it a part of the radiation system. The AUT to be in an offset position relative to the measurement center is general. Fortunately, offset measurements and proper NF/FF transformation processing can yield an accurate far-field radiation pattern [6-8]. Thus, this section uses the offset measurement scheme, and the simulation structure as shown in Fig. 4.

A. Simulation Environment Setup

Although the results of offset NF measurement for different DUTs may vary, the impact of the offset configuration on the measurement system is generally similar. In this study, a rectangular horn antenna with a wide operating band is used as the DUT, with a center frequency of 3 GHz. The offset configuration is set as follows: the DUT is placed in the horizontal xoy plane along the x-axis direction, with an offset distance of 2 meters, and a measurement distance of 5 meters. The sampling points on the measurement sphere are assumed to be equally spaced (constant $\Delta\theta$ and $\Delta\varphi$ angular sampling step). During the simulation process, the probe rotates on a spherical surface centered at the coordinate system (measurement center), collecting data across the entire surface to simulate the actual measurement process.

B. Simulation Content Design

In an ideal scenario, the theoretical calculation of the radiation power at the sampling points in the NF during the normal operation of the DUT is obtained through simulation software. Subsequently, the spherical NF data is transformed into FF data using the NF/FF transformation algorithm mentioned in [6]. This set of data will serve as the ideal near-field to far-field transformation data (ideal NF2FF) in this paper. Theoretical values of electromagnetic wave power radiated by the DUT in the FF region are obtained through numerical calculations under the same conditions. This set of data will serve as the ideal far-field data (ideal FF) in this paper. However, the ideal NF2FF is subject to certain errors due to data truncation by the computer and the limited accuracy of the NF/FF transformation algorithm. Finally, two sets of data are obtained according to the radiation performance of the DUT, as shown in Fig. 5, and both have been normalized for comparison. This comparison will verify whether the accuracy of the NF/FF transformation algorithm used in the current testing system meets the requirements. The ideal FF data is selected as the reference data for the simulation, which is entirely based on theoretical calculations and is considered an accurate value without any errors. Therefore, the reference data is set as the evaluation standard for the subsequent simulation results. The difference between the actual simulation results and the reference data is considered as the measurement error of the probe, which is only related to the performance indexes of the probe antenna itself.

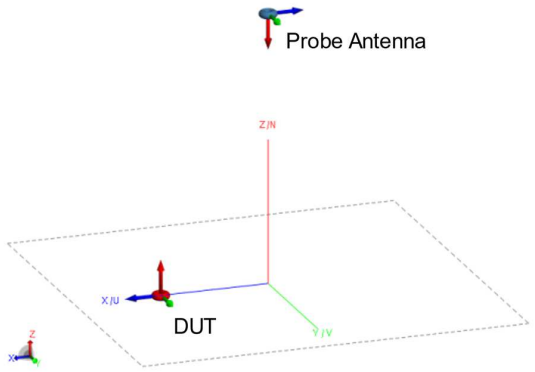

Fig. 4.Offset measurement simulation structure

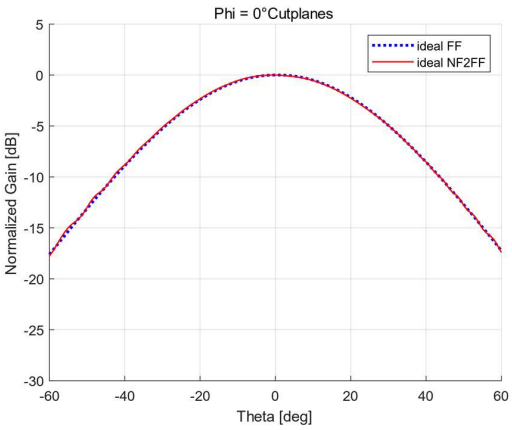

Fig. 5.DUT's far-field pattern of radiated power

In the actual simulations, the S_{21} parameter represents the transmission parameter from the measurement probe port to the DUT port and can be used to simulate the sampled data in the NF. Then the NF data is converted into the final simulation results through the NF/FF transformation algorithm. For comparison purposes, this paper uses the following standards: Results are only compared within the range of ± 20 degrees of pitch angle, which totals 40 degrees, to avoid the influence of edge data cutoff errors. Additionally, the half-power beam width of the probe antenna should better meet the 40-degree angle condition. Secondly, the error between the calculated results and the reference data should be less than 0.5 dB. A smaller error indicates stronger probe performance. It is assumed that if the error exceeds the limit, the measurement requirements cannot be met.

To research potential issues resulting from insufficient probe indexes under offset configuration, we select several commonly used OTA probe antennas for simulation, including the rectangular horn (rhorn), double ridged horn (ridge), corrugated horn (chorn), and Vivaldi antenna (vivaldi). The test frequency is set to 3 GHz, and the test environment layout is consistent with the aforementioned offset configuration. The physical models of these probe antennas are depicted in Fig. 6-9. TABLE I presents the indexes of the existing probe antennas, which mainly include three radiation performance indicators: half-power beam width (3 dB width), beam symmetry (roundness difference of the power pattern on the measurement plane), and in-band cross-polarization.

TABLE I. Indexes of commonly used OTA probe antennas

Type	*Probe Antenna Indexes*		
	3dB Width (deg)	***Symmetry (dB)***	***Cross Polarization (dB)***
rhorn	28.80	1.29	33.80
ridge	33.73	1.37	47.06
chorn	65.88	0.59	28.68
vivaldi	49.22	1.34	36.68

C. Simulation Results Discussion and Analyzation

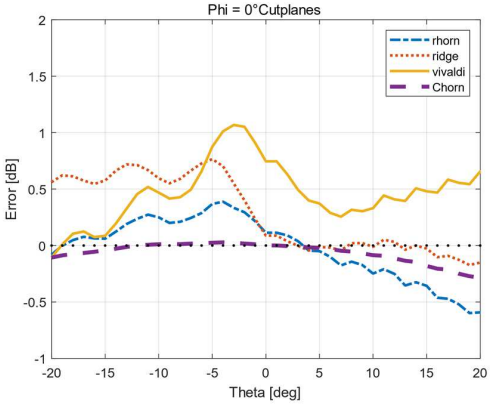

Fig. 10.Near-field calculated error curve of existing probe antennas

Fig. 10 displays the error between simulation results and reference data of four existing probe antennas. Upon comparison of the simulation data, it can be inferred that the rectangular horn and double ridged horn have errors greater than 0.5 dB at 40 degrees. This is mainly because the half-power beam width (less than 40°) does not sufficiently cover the NF sampling range under offset configuration. The beam symmetry index of the probe antenna within the beam width range is also critical. For example, the Vivaldi antenna has a poor beam symmetry index, which is 1.34 dB. Even though the beam width is greater than 40 degrees, the simulation error reaches 1.06 dB. Although the corrugated horn can meet the comparison standard of 0.5 dB at the specified test frequency, its primary issue is insufficient working bandwidth. The design of the corrugated horn antenna faces a challenging objective in meeting the bandwidth of 0.45 GHz-6 GHz (ultrawide band with a relative bandwidth exceeding 170%).

IV. Challenge and Prospect of Vehicle OTA Probe Antenna

In the design experiment of this paper, the corrugated horn antenna performed close to expectations. However, it still faces the challenge of limited working bandwidth when compared to the measurement requirements. In general, as the frequency increases, the antenna directivity D also increases [6], as shown in (5). However, in simpler terms, increasing directivity means reducing the beam width ($D = 40000/\theta_E\theta_H$) [6]. Consequently, the antenna struggles to maintain a constant beam width across high and low frequencies. Therefore, the problem of OTA spherical near-field measurement of large devices such as vehicles remains

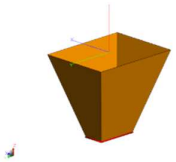

Fig. 6.Rectangular horn

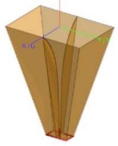

Fig. 7.Double ridged horn

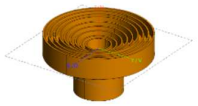

Fig. 8.Corrugated horn

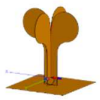

Fig. 9.Vivaldi antenna

unresolved. To meet the growing demand, it is critical to design a probe antenna with a wide working bandwidth, broad

$$D = 4\pi S\frac{f^2}{c^2} \tag{5}$$

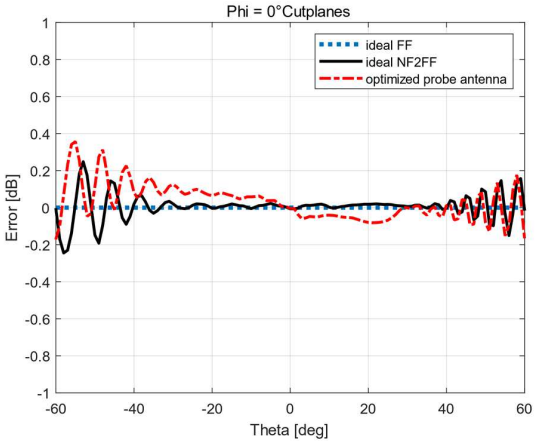

Fig. 11.Calculated error curve of probe antenna

TABLE II. Indexes of optimized probe antenna

Optimized Probe Antenna Indexes		
Distance: 5 meters		*Offset: 2 meters*
3dB Width (deg)	*Symmetry (dB)*	*Cross Polarization (dB)*
65.00	0.60	30.00

beam coverage, and good beam symmetry.

The simulation software is used to establish the radiation pattern of the optimized probe, and a large number of simulations are conducted to continuously adjust the three indicators of the probe: beam width, symmetry, and cross polarization. Through this process, a group of excellent simulation results are obtained. Fig. 11 shows the error curve between the simulation results of this optimized probe and the reference data. Similarly, a 40-degree measurement angle is selected for comparative analysis. With this set of performance indexes, the optimized probe can achieve measurement error that meets the comparison standard set in this paper. The main performance indexes of the optimized probe are shown in TABLE II.

The results presented in this paper are obtained through simulation software. Since the simulation results are based on the NF/FF transformation algorithm, it is difficult to draw conclusions from the formula derivation method alone. However, the simulation data does provide evidence that the three probe performance indexes have a significant impact on the NF measurement results under the offset configuration. Therefore, studying the probe performance index is crucial to meet the growing demand for offset NF measurement. Subsequent papers will present detailed formula derivation and measurement work.

Therefore, based on the results of the simulation, recommended values for the performance index of the optimized probe under the offset configuration are provided. The half-power beam width is recommended to be larger than 65 degrees, and the larger it covers, the smaller the sampling error will be. Beam symmetry is recommended to be less than 0.6 dB. The cross-polarization performance of the antenna exhibits good performance in the simulation with the polarization component being less than -30 dB, and hence, its impact can be ignored. However, in practical engineering, the cross-polarization performance can easily be affected by beam symmetry and manufacturing processes. To reduce uncertainty caused by polarization mismatch, the cross-polarization performance in the band should be intensified as much as possible.

V. Conclusion

This paper explores the issue of performance indexes for NF measurement probes used in the offset scenario of large DUTs. The paper also highlights the universality of the offset configuration in NF measurement systems. To simulate NF measurement, an offset configuration is employed, and ideal FF data is used as a reference. By comparing the simulation results of the reference data, the measurement error of the probe is determined. Several commonly used OTA NF measurement probe performances are compared and analyzed using this error definition. Based on the analysis, all three performance indexes of the probe impact the NF measurement results under the offset configuration. The half-power beamwidth is identified as one of the main causes of sampling errors in the NF measurement system. To obtain an optimized probe that meets the NF measurement requirements for large automobiles under the offset configuration, the radiation pattern of the probe is continuously adjusted through multiple simulations. The main performance indexes of the probe are presented in TABLE II of the paper. All the data in the table are obtained from simulations, and this set of data is recommended as the performance benchmark for NF measurement probes under the aforementioned offset configuration.

Acknowledgment

This work was supported by the National Key R&D Program of China under Grant 2022YFF0604804.

References

[1] O. Breinbjerg, "Spherical near-field antenna measurements — the most accurate antenna measurement technique," 2016 IEEE Int. Symp. Antennas Propag. pp. 1019-1020, 2016.

[2] L. J. Foged, F. Saccardi, F. Mioc and P. O. Iversen, "Spherical near field offset measurements using downsampled acquisition and advanced NF/FF transformation algorithm", Proc. 10th Eur. Conf. Antennas Propag. (EuCAP), pp. 1-3, Apr. 2016.

[3] Rasmus Cornelius, Dirk Heberling, "Spherical wave expansion with arbitrary origin for near-field antenna measurements", IEEE Trans. Antennas Propag, vol.65, no.8, pp. 4385-4388, Aug. 2017.

[4] Francesco Saccardi, Francesca Mioc, Per O. Iversen, Lars J. Foged, "Application of the TSWE algorithm to echo reduction of under-sampled offset spherical near-field measurements", IET Microw, Antennas & Propag, vol.12, no.4, pp.549-553, 2018.

[5] F. Wollenschläger, L. J. Foged, M. E. Asghar, C. Bornkessel and M. A. Hein, "Spherical wave expansion applied to the measured radiation patterns of automotive antennas in the installed state in the GHz range," Proc. 13th Eur. Conf. Antennas Propag, (EuCAP), Krakow, Poland, pp. 1-5, 2019.

[6] J. Hansen, Ed., Spherical Near-field Antenna Measurements. London, U.K.: Peter Peregrinus, Ltd., 1988.

[7] ANSI/IEEE Std 149-1979 "IEEE Standard Test Procedures for Antennas"

[8] IEEE Std P1720™/D2 (Draft) "Recommended Practice for Near-Field Antenna Measurements"